Comparison of the Temperature and Location Dependence of ^1H and ^{13}C NMR Shifts between Saturated 1,3- and 1,2-Diamines Coordinated to Low-Spin Tetracyanoferrate(III)

Yoshitaka KURODA,* Masafumi GOTO,*,† and Tomoya SAKAI
Faculty of Pharmaceutical Sciences, Nagoya City University, Mizuho-ku, Nagoya 467
†Faculty of Pharmaceutical Sciences, Kumamoto University, Kumamoto 862
(Received November 26, 1990)

The temperature dependence of the ^1H NMR for low-spin iron(III) complexes, $[Fe^{III}(CN)_4(1,3\text{-diamine})]^-$, with 1,3-propanediamine, (2*R*,4*S*)-2,4-pentanediamine, and (2*R*,4*R*)-2,4-pentanediamine were measured at 323—183 K. The coordinated amine segment, $Fe\text{–}N(H_N)_2\text{–}C(H_\alpha)_2\text{–}C(H_\beta)_2$, resonated in the following magnetic field regions at 323—183 K: H_α^{ax}, 7.2—20.5; H_β^{ax}, 10.8—35.0; H_β^{eq}, 23.9—65.7; H_β^{methyl}, 1.8—9.9 ppm. All of the ^1H signals moved in the downfield direction with a decrease in the temperature, and exhibited a non-Curie behavior. The H_N shifts at 300 K were 110—279 ppm. The temperature and location dependence of the isotropic shift (δ^{iso}) for the ^1H and ^{13}C nuclei were accounted for by the combination of Fermi contact and dipolar contributions. The Fermi constants and spin populations were estimated for the ^1H and ^{13}C nuclei. Not only the spin polarization mechanism, but also a direct mechanism, were suggested for spin propagation from the Fe^{III} to the respective atoms.

Paramagnetic metal ions affect the NMR shifts of the compounds coordinated to them.[1] Such effects of metal ions have heen extensively investigated for unsaturated compounds.[2,3] On the other hand, studies of saturated compounds have almost been limited to Ni^{II} amine complexes.[4–7] Transition metal ions, such as the low-spin Fe^{III} ion, are expected to have different magnetic effects from those of Ni^{II}, according to their electronic configurations.

The ^1H and ^{13}C NMR spectra of saturated 1,2-diamines coordinated to a low-spin Fe^{III} ion, $[Fe^{III}(CN)_4(1,2\text{-diamine})]^-$, have been studied by using 1,2-ethanediamine (en), (*R*)-1,2-propanediamine (*R*-pn), (1*R*,2*R*)-1,2-cyclohexanediamine (*R*-chxn), *N*,*N*′-dimethyl-1,2-ethanediamine (s-Me$_2$en), etc.[8–10]

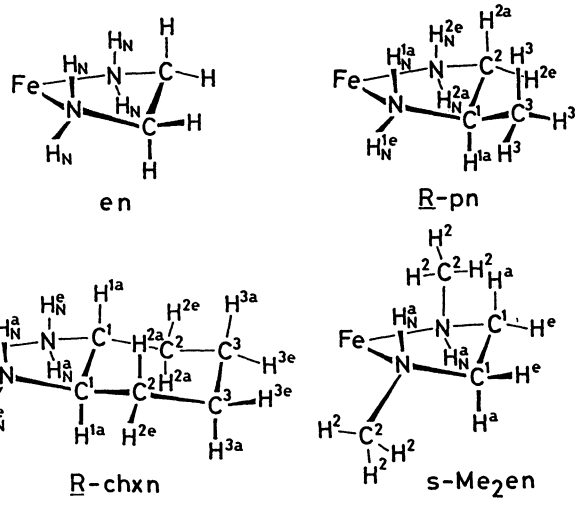

These Fe^{III} complexes do not obey the Curie law and show characteristic isotropic shifts (δ^{iso}) which are strongly dependent on the nuclear locations relative to the paramagnetic center, the Fe^{III} ion: downfield and upfield shifts were observed for the axial and equatorial protons bonded to the same carbon atom on the chelate ring, respectively. To clarify these features, δ^{iso} was separated into the Fermi contact shift (δ^{con}) and the dipolar shift (δ^{dip}), based on the electronic states obtained from a *g*-value analysis of the Fe^{III} en complex;[9] these shifts have been related to the nuclear positions.[9,10] This investigation has revealed that (1) nuclei nearer to the average plane of the chelate ring have larger δ^{con} values, and (2) that the non-Curie behavior of δ^{iso} can be accounted for by the temperature dependence of δ^{dip}.

The 1,3-diamine chelates, $[Fe^{III,II}(CN)_4(1,3\text{-diamine})]^{-,2-}$, such as (2*R*,4*S*)-2,4-pentanediamine (*meso*-ptn), 1,3-propanediamine (tn), (2*R*,4*R*)-2,4-pentanediamine (*R*-ptn), and 1,3-butanediamine (1,3-bn) assume a chair or skew-boat conformation, as shown in Fig. 1.[11] These 1,3-diamine chelates have a central methylene part which is absent in the 1,2-diamine chelates, and the nuclei of the former are further apart from the coordination plane than those of the latter with *gauche* conformations.[12–15] These structural differences are expected to make the δ^{dip} and δ^{con} values for the 1,3-diamine chelates different from those for the 1,2-diamine chelates.

The variations of the ^1H NMR shifts of the 1,3-diamine chelates with temperature were previously utilized for estimating the chair⇆chair interconversion rate,[16] though the temperature dependence was treated empirically. We now report on the $C^1\underline{H}$ and $N^1\underline{H}$ shifts of the *meso*-ptn, tn, *R*-ptn, and 1,3-bn chelates measured at 323—183 and 300 K, respectively. The δ^{iso} values for the C<u>H</u> and N<u>H</u> shifts, as well as the previously reported ^{13}C shifts,[11] are separated into δ^{dip} and δ^{con}. The δ^{con} values, thus obtained, are compared with those for the Fe^{III} 1,2-diamine chelates.[9,10]

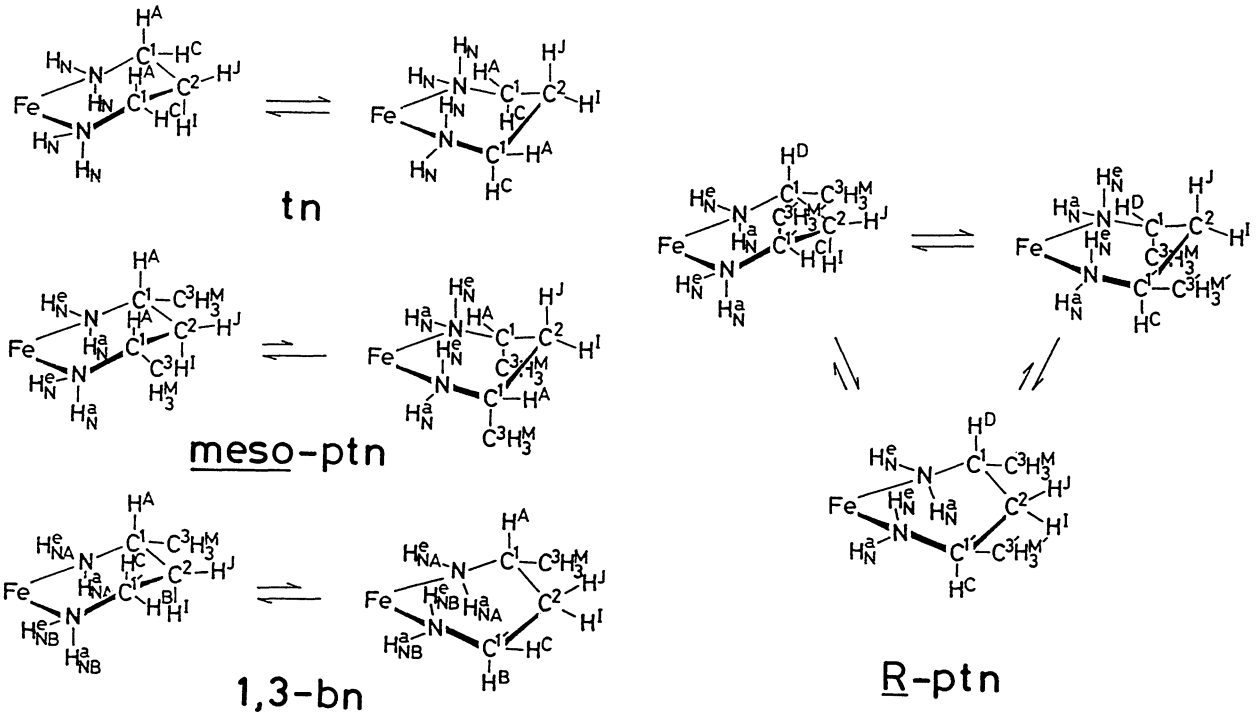

Fig. 1. Schematic structures of the chelates and the numbering of protons and carbons. Fe=Fe(CN)$_4$.

Experimental

Materials. Sodium tetracyano(1,3-diamine)ferrate(III) and ferrate(II) complexes containing 1,3-propanediamine (tn), (2*R*,4*S*)-2,4-pentanediamine (*meso*-ptn), (2*R*,4*R*)-2,4-pentanediamine (*R*-ptn), and 1,3-butanediamine (1,3-bn) as 1,3-diamines were prepared as previously reported.[11]

Measurement. The variable-temperature ^{1}H NMR spectra of the Fe^{III} 1,3-diamine complexes were recorded on a JEOL FX-100 spectrometer with ca. 0.05 M (1 M=1 mol dm^{-3}) solutions in CD_3OD containing 0.25% DCl at 323—183 K. Acidic solutions were necessary to protect the coordinated diamines against dehydrogenation.[17,18] Dilute solutions were required in order to avoid the deposition of complexes below 273 K. FID signals (pulse width: 7 μs; observation time 10 s) were collected 40 times for each sample at each temperature to obtain spectra with S/N ratios over 20/1. The probe temperature was controlled with a JNM-VT-3C temperature-control apparatus, and determined from the chemical shift difference between the methyl and hydroxyl protons of methanol.[19] The N^{1}H shifts of the Fe^{III} 1,3-diamine complexes were recorded on a JEOL FX-100 spectrometer at 300 K using 40—50 mg of the complexes dissolved in pD 2.0 DCl–D_2O (0.3 cm^3). Sodium 3-trimethylsilylpropionate-2,2,3,3-d_4 (TSP; 0.00 ppm) was used as an internal reference. The positive chemical shifts indicate downfield shifts from the standard.

Results and Discussion

Temperature Dependence of ^{1}H NMR Spectra of $[Fe^{III}(CN)_4(1,3\text{-diamine})]^-$. ^{1}H NMR spectra of $[Fe^{III}(CN)_4(tn)]^-$, $[Fe^{III}(CN)_4(meso\text{-ptn})]^-$, and $[Fe^{III}(CN)_4(R\text{-ptn})]^-$ (tn=1,3-propanediamine, *meso*-ptn=(2*R*,4*S*)-2,4-pentanediamine, *R*-ptn=(2*R*,4*R*)-2,4-pentanediamine) were measured in CD_3OD containing 0.25% DCl. The temperature range was limited to 323—183 K by the boiling and freezing points of the solvent.[16,20] Acidification of the solvent with DCl is necessary to protect the coordinated diamine molecule against dehydrogenation, which yields the corresponding Fe^{II} diimine complex under neutral or basic conditions.[17,18] The observed chemical shifts ($\delta_{Fe^{III}}$) are listed in the fifth column of Table 1.

(a) *meso*-ptn. $[Fe^{III}(CN)_4(meso\text{-ptn})]^-$ showed four CH peaks of H^J, H^I, H^A, and H^M downfield, with an area ratio of 1:1:2:6.[11] These peaks moved in the downfield direction and dispersed with a decrease in temperature. Their line-widths at half-height were broadened from 29, 47, 63, and 17 Hz at 323 K to 210, 350, 530, and 105 Hz at 183 K, respectively.

The large difference in the $\delta_{Fe^{III}}$ values of H^I and H^J, i.e. ca. 13—31 ppm at 323—183 K, indicates that the *meso*-ptn chelate is fixed in a chair conformation with two equatorial methyl groups (See Fig. 1). The H^A shift is less than the H^I and H^J shifts, whereas the corresponding axial protons of the 1,2-diamine chelates show the largest downfield shift among the CH's.[9,10,16,20] The H^A and H^M shifts are less than half the corresponding shifts for the 1,2-diamine chelates. The line-width at half-height is of the order of $H^A > H^I > H^J > H^M$, the reversed order of their distance from the Fe^{III} ion.

(b) tn. $[Fe^{III}(CN)_4(tn)]^-$ exhibited two peaks, one downfield and the other upfield, with an area ratio of 1:2. The former was assigned to H^I and H^J, and the latter to H^A and H^C. The $H^{I,J}$ shift is almost the same as the mean of the H^I and H^J shifts for the *meso*-ptn

Table 1. ^1H and ^{13}C NMR Shifts[a] and Calculated Isotropic, Dipolar, and Fermi Contact Shifts[a] for $[Fe^{III}(CN)_4(1,3\text{-diamine})]^-$

Diamine	Nucleus	Temp	$\delta_{Fe^{II}}$[b]	$\delta_{Fe^{III}}$	δ^{iso}[c]	δ^{dip}[d]	δ^{con}[e]
		K	ppm	ppm	ppm	ppm	ppm
tn	$H^{A,C}$	323	—	−6.00	−8.80	7.17	−15.97
		313	—	−6.06	−8.86	7.65	−16.51
		303	2.80	−6.15	−8.95	8.17	−17.12
		293	—	−6.19	−8.99	8.75	−17.74
		283	—	−6.27	−9.07	9.38	−18.45
		273	—	−6.34	−9.14	10.08	−19.22
		263	—	−6.44	−9.24	10.85	−20.10
		253	—	−6.53	−9.33	11.71	−21.04
		243	—	−6.65	−9.45	12.66	−22.11
		233	—	−6.80	−9.60	13.72	−23.32
		223	—	−6.97	−9.77	14.91	−24.68
		213	—	−7.09	−9.89	16.24	−26.13
		203	—	−7.21	−10.01	17.74	−27.75
		193	—	−7.36	−10.16	19.43	−29.59
		183	—	−7.62	−10.42	21.35	−31.77
	$H^{I,J}$	323	—	18.17	16.74	12.14	4.60
		313	—	19.05	17.62	12.95	4.67
		303	1.43	20.08	18.65	13.84	4.81
		293	—	21.33	19.90	14.81	5.09
		283	—	22.59	21.16	15.88	5.28
		273	—	24.08	22.65	17.07	5.58
		263	—	25.55	24.12	18.37	5.75
		253	—	27.65	26.22	19.82	6.40
		243	—	29.57	28.14	21.44	6.70
		233	—	32.24	30.81	23.23	7.58
		223	—	34.80	33.37	25.24	8.13
		213	—	37.72	36.29	27.50	8.79
		203	—	41.37	39.94	30.04	9.90
		193	—	45.49	44.06	32.90	11.16
		183	—	50.93	49.50	36.15	13.35
	H_N	300	f)	193.0	193.0	7.9	185.1
	C^1	300	42.3[g]	222.4[g]	180.1	23.0	157.1
	C^2	300	28.6[g]	29.4[g]	0.8	22.9	−22.1
meso-ptn	H^A	323	—	7.23	4.43	2.63	1.80
		313	—	7.55	4.75	2.81	1.94
		303	2.80	7.89	5.09	3.00	2.09
		293	—	8.31	5.51	3.21	2.30
		283	—	8.80	6.00	3.45	2.55
		273	—	9.24	6.44	3.70	2.74
		263	—	9.83	7.03	3.99	3.04
		253	—	10.52	7.72	4.30	3.42
		243	—	11.20	8.40	4.65	3.75
		233	—	12.11	9.31	5.04	4.27
		223	—	13.21	10.41	5.47	4.94
		213	—	14.51	11.71	5.96	5.75
		203	—	15.81	13.01	6.51	6.50
		193	—	17.77	14.97	7.14	7.83
		183	—	20.49	17.69	7.84	9.85
	H^I	323	—	10.83	9.95	7.92	2.03
		313	—	11.52	10.64	8.45	2.19
		303	0.88	12.20	11.32	9.03	2.29
		293	—	13.04	12.16	9.67	2.49
		283	—	13.92	13.04	10.37	2.67
		273	—	14.98	14.10	11.14	2.96
		263	—	16.10	15.22	11.99	3.23
		253	—	17.45	16.57	12.94	3.63
		243	—	18.80	17.92	13.99	3.93
		233	—	20.54	19.66	15.17	4.49
		223	—	22.75	21.87	16.48	5.39
		213	—	25.12	24.24	17.95	6.29
		203	—	27.77	26.89	19.60	7.29
		193	—	30.71	29.83	21.48	8.35
		183	—	34.95	34.07	23.60	10.47
	H^J	323	—	23.85	22.23	16.85	5.38
		313	—	25.07	23.45	17.97	5.48
		303	1.62	26.30	24.68	19.20	5.48
		293	—	27.82	26.20	20.56	5.64
		283	—	29.41	27.79	22.04	5.75
		273	—	31.28	29.66	23.69	5.97
		263	—	33.31	31.69	25.50	6.19
		253	—	35.71	34.09	27.51	6.58
		243	—	38.07	36.45	29.75	6.70
		233	—	41.15	39.53	32.24	7.29
		223	—	44.95	43.33	35.03	8.30
		213	—	49.07	47.45	38.16	9.29
		203	—	53.34	51.72	41.69	10.03
		193	—	58.60	56.98	45.66	11.32
		183	—	65.66	64.04	50.17	13.87
	H^M	323	—	2.52	1.31	3.64	−2.33
		313	—	2.72	1.51	3.89	−2.38
		303	1.21	2.94	1.73	4.16	−2.43
		293	—	3.21	2.00	4.45	−2.45
		283	—	3.48	2.27	4.77	−2.50
		273	—	3.79	2.58	5.13	−2.55
		263	—	4.14	2.93	5.52	−2.59
		253	—	4.56	3.35	5.96	−2.61
		243	—	4.96	3.75	6.44	−2.69
		233	—	5.56	4.35	6.98	−2.63
		223	—	6.15	4.94	7.58	−2.64
		213	—	6.86	5.65	8.26	−2.61
		203	—	7.62	6.41	9.02	−2.61
		193	—	8.60	7.39	9.89	−2.50
		183	—	9.93	8.72	10.86	−2.14
	H_N^a	300	f)	110.2	110.2	21.8	88.4
	H_N^c	300	f)	278.8	278.8	0.7	278.1
	C^1	300	49.8[g]	214.9[g]	165.1	20.9	144.2
	C^2	300	43.2[g]	50.8[g]	7.6	23.0	−15.4
	C^3	300	26.7[g]	−35.9[g]	−62.6	6.3	−68.9
R-ptn	$H^{C,D}$	323	—	−0.29	−3.29	10.29	−13.58
		313	—	−0.15	−3.15	10.97	−14.12
		303	3.00	−0.12	−3.12	11.72	−14.84
		293	—	0.32	−2.68	12.55	−15.23
		283	—	0.53	−2.47	13.46	−15.93
		273	—	0.88	−2.12	14.46	−16.58
		263	—	1.12	−1.88	15.57	−17.45
		253	—	1.44	−1.56	16.80	−18.36
	$H^{I,J}$	323	—	14.18	12.74	10.13	2.61
		313	—	14.83	13.39	10.81	2.58
		303	1.44	15.42	13.98	11.55	2.43
		293	—	16.57	15.13	12.36	2.77
		283	—	17.53	16.09	13.25	2.84
		273	—	18.63	17.19	14.24	2.95
		263	—	19.92	18.48	15.33	3.15
		253	—	21.27	19.83	16.54	3.29
		243	—	22.89	21.45	17.89	3.56
		233	—	24.92	23.48	19.38	4.10
		223	—	26.92	25.48	21.06	4.42
		213	—	29.48	28.04	22.94	5.10
		203	—	32.37	30.93	25.06	5.87

Table 1. (Continued)

Diamine	Nucleus	Temp K	$\delta_{Fe^{II}}$ [b] ppm	$\delta_{Fe^{III}}$ ppm	δ^{iso} [c] ppm	δ^{dip} [d] ppm	δ^{con} [e] ppm
		193	—	35.57	34.13	27.45	6.68
		183	—	40.19	38.75	30.16	5.59
	H^M	323	—	1.77	0.62	3.79	−3.17
		313	—	1.88	0.73	4.04	−3.31
		303	1.15	1.97	0.82	4.32	−3.50
		293	—	2.12	0.97	4.62	−3.65
		283	—	2.27	1.12	4.95	−3.83
		273	—	2.38	1.23	5.32	−4.09
		263	—	2.54	1.39	5.73	−4.34
		253	—	2.68	1.53	6.18	−4.65
		243	—	2.82	1.67	6.68	−5.01
		233	—	3.03	1.88	7.25	−5.37
		223	—	3.44	2.29	7.87	−5.58
		213	—	3.55	2.40	8.58	−6.18
		203	—	3.68	2.53	9.37	−6.84
		193	—	3.79	2.64	10.26	−7.62
		183	—	3.96	2.81	11.28	−8.47
	H^a_N	300	f)	134.0	134.0	14.6	119.4
	H^c_N	300	f)	231.1	231.1	0.1	231.0
	C^1	300	44.9[g]	216.3[g]	171.4	26.3	145.1
	C^2	300	40.3[g]	46.9[g]	6.6	22.4	−15.8
	C^3	300	25.5[g]	−21.0[g]	−46.5	7.1	−53.6
1,3-bn	H^a_{NA}	300	f)	106.9	106.9	21.8	85.1
	H^a_{NB}	300	f)	118.8	118.8	21.8	97.0
	H^c_{NA}	300	f)	274.9	274.9	0.7	274.2
	H^c_{NB}	300	f)	268.8	268.8	0.7	268.1
	H^A	300	2.92[g]	6.30[g]	3.38	3.07	0.31
	H^B	300	2.91[g]	−11.35[g]	−14.26	7.10	−21.36
	H^C	300	2.65[g]	5.73[g]	3.08	3.07	0.01
	H^I	300	1.03[g]	14.64[g]	13.61	9.23	4.38
	H^J	300	1.62[g]	32.70[g]	31.08	19.62	11.46
	H^M	300	1.24[g]	3.97[g]	2.73	4.25	−1.52
	C^1	300	42.4[g]	202.9[g]	160.5	20.9	139.6
	$C^{1'}$	300	49.4[g]	239.8[g]	190.4	20.9	169.5
	C^2	300	35.7[g]	39.5[g]	3.8	23.0	−19.2
	C^3	300	26.7[g]	−39.4[g]	−66.1	6.3	−72.4

a) Positive values indicate downfield shifts. b) Chemical shifts for $[Fe^{II}(CN)_4(diamine)]^{2-}$ were measured in D_2O at 300 K.[11] c) Isotropic shifts calculated from Eqs. 1—3. d) Dipolar shifts calculated from Eq. 2. e) Fermi contact shifts calculated from Eq. 3. f) The NH signal for $[Fe^{II}(CN)_4(meso\text{-ptn})]^{2-}$ was observed at 2.16 ppm in pD 2.0 DCl-D_2O solution. Since this shift is small enough compared with $\delta_{Fe^{III}}$, we assumed that δ^{con} is equal to $\delta_{Fe^{III}}$. g) From Ref. 11.

chelate in the 323—183 K temperature range.[11] This signal-averaging indicates a rapid interconversion of the tn chelate between the two chair forms (See Fig. 1), the rate constant of which has been already estimated to be 6×10^8 s^{-1} at 298 K.[16]

The magnitude of the $H^{I,J}$ shifts is larger than that of the $H^{A,C}$ shifts, despite the longer distances between the former nuclei and the Fe^{III} ion. This order of $\delta_{Fe^{III}}$ is different from that for the 1,2-diamine chelates, where the nuclei nearer the Fe^{III} ion have shown larger $\delta_{Fe^{III}}$ values.[8-10]

As the temperature decreased, the magnitude of the $H^{A,C}$ and $H^{I,J}$ shifts increased. The $H^{A,C}$ peak was wider than the $H^{I,J}$ peak: The line-widths at half-height were 36 and 27 Hz at 323 K, and 590 and 470 Hz at 183 K, respectively. This broadening with a decrease in the temperature is due to a rapid exchange of the resonance sites, in addition to a reduction of the relaxation time. The expected four peaks corresponding to H^A, H^C, H^I, and H^J, however, could not be observed, even at 183 K.

(c) *R*-ptn. $[Fe^{III}(CN)_4(R\text{-ptn})]^-$ showed three signals of $H^{I,J}$, H^M, and $H^{C,D}$ downfield with an area ratio of 1:3:1. This signal-averaging is attributable to an alteration of the *R*-ptn chelate between the chair and λ-skew-boat forms shown in Fig. 1.[11] The population of the two forms has been estimated to be ca. 50:50, based on the $H^{C,D}$ shift at 300 K.[11]

All of the signals moved in the downfield direction as the temperature decreased. The overlap with the solvent signals prevented any observation of the $H^{C,D}$ signal below 243 K. The widths of the $H^{I,J}$, H^M, and $H^{C,D}$ peaks were 21, 18, and 62 Hz at 323 K, respectively. The decrease in the temperature to 183 K broadened these peaks, but was not sufficient to separate them into the peaks corresponding to the individual protons. The *R*-ptn chelate is, thus, expected to alter between the chair and λ-skew-boat forms as fast as the tn chelate, i.e. $>10^8$ s^{-1} at 298 K.[16]

The ^1H shifts of these Fe^{III} 1,3-diamine complexes are plotted against T^{-1} in Fig. 2. The nonlinearity indi-

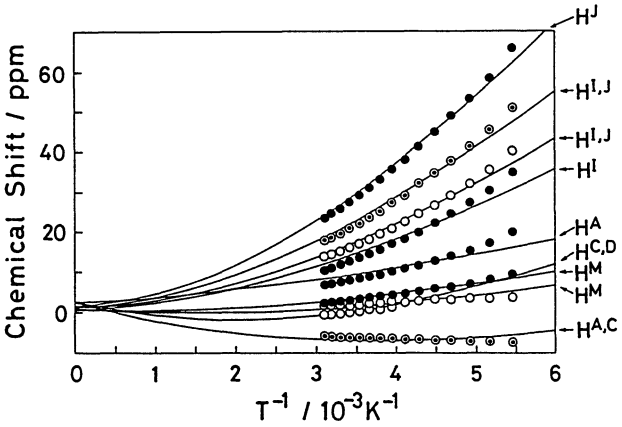

Fig. 2. Temperature dependence of ^1H NMR shifts of $[Fe^{III}(CN)_4(1,3\text{-diamine})]^-$ in CD_3OD containing 0.25% DCl. The circles indicate the observed values: *meso*-ptn (●), tn (⊙), and *R*-ptn (○). The solid curves indicate the estimated values. The chemical shifts at $T^{-1}=0$ are the shifts of the corresponding Fe^{II} complexes.

cates that the 1,3-diamine chelates, as well as the 1,2-diamine chelates,[9,10,20] do not obey the Curie law.

Amino Protons. The ^1H NMR spectra of the amino protons (NH) of $[Fe^{III}(CN)_4(1,3\text{-bn})]^-$ (1,3-bn=1,3-butanediamine), besides the Fe^{III} 1,3-diamine complexes described above, were measured in p*D* 2.0 DCl–D_2O at 300 K. The following chemical shifts and line-widths at half-height were obtained: *meso*-ptn, 110.2 (390) and 278.8 (840); tn, 193.0 (510); *R*-ptn, 134.0 (160) and 231.1 (320); 1,3-bn, 106.9 (580), 118.8 (580), 268.8 (820), and 274.9 ppm (950 Hz). The higher field peaks were assigned to the axial amino protons and the lower field peaks to the equatorial protons, as those for the 1,2-diamine complexes.[10]

The two NH peaks observed for the *meso*-ptn chelate correspond to H_N^a and H_N^e (See Fig. 1). The $\delta_{Fe^{III}}$ difference of the NH peaks amounts to 168.6 ppm, which is ca. 5 times as large as 34 ppm for the *R*-chxn chelate.[10] This large difference indicates that the *meso*-ptn chelate assumes a chair form.

The single NH peak for the tn chelate has almost the same values of chemical shift and line-width as the mean values, 194.5 ppm and 560 Hz, for the H_N^a and H_N^e peaks of the *meso*-ptn chelate. The rapid interconversion of the tn chelate between the two chair forms is, thus, demonstrated by the NH as well as CH line shapes.

The difference between the two NH shifts of the *R*-ptn chleate, 97.1 ppm, is 58% of that for the *meso*-ptn chelate, and the average NH shift of the former differs by ca. 10 ppm from those for the *meso*-ptn and tn chelates. These features are ascribed to a rapid chair$\leftrightarrows$ λ-skew-boat alteration of the *R*-ptn chelate.[11] If the λ-skew-boat form is assumed to have the same NH shift difference, 34 ppm, as the 1,2-diamine chelates, the estimated ratio of the chair : λ-skew-boat is ca. 53 : 47. This ratio is almost the same as that reported for $[Ni(H_2O)_4(rac\text{-ptn})]^{2+}$, 54 : 46.[4]

The 1,3-bn chelate exists as an equilibrium mixture of a chair and a skew-boat form with an equatorial methyl group.[11] The population of the chair form has been estimated to be 76—96% from the $H^B$and H^Cshifts,[11] whereas 98% is obtained from the H^A shift (see Table 1). This difference indicates that the conformation at the methyl group-side resembles that of the *meso*-ptn chelate, while the unsubstituted methylene has a different conformation from that of the latter. The four NH peaks were assigned, from downfield to upfield, to H_{NA}^a, H_{NB}^a, H_{NB}^e, and H_{NA}^e, by comparing the NH shifts of the 1,3-bn and *meso*-ptn chelates.

The typical values of $\delta_{Fe^{III}}$ and the line-width for H_N^a

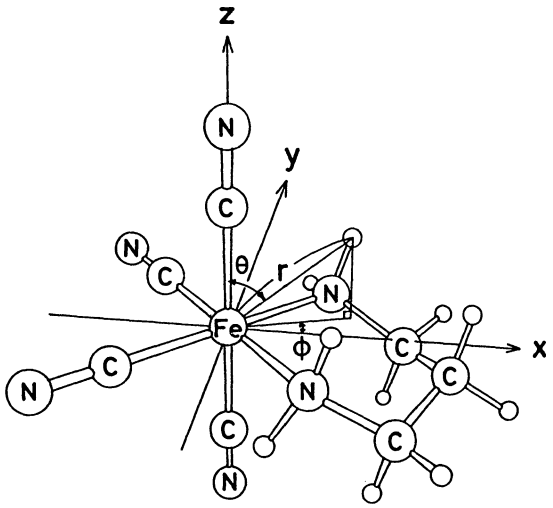

Fig. 3. Coordinate system for the analysis of isotropic NMR shift.

Table 2. Geometric Factors

Diamine	Nucleus	G_A	G_B	Diamine	Nucleus	G_A	G_B
		10^{28} m^{-3}	10^{28} m^{-3}			10^{28} m^{-3}	10^{28} m^{-3}
tn	H_N	−4.898	−2.011	*meso*-ptn	H_N^a	−3.733	1.284
	$H^{A,C}$	−0.842	0.908		H_N^e	−6.391	−4.611
	$H^{I,J}$	−1.421	1.540		H^A	0.485	0.890
	C^1	−2.864	2.117		H^I	−0.821	1.080
	C^2	−2.374	2.446		H^J	−2.054	2.080
1,3-bn	H_{NA}^a	−3.733	1.284		H^M	−0.812	0.193
	H_{NB}^a	−3.733	1.284		C^1	−2.560	1.950
	H_{NA}^e	−6.391	−4.611		C^2	−2.267	2.532
	H_{NB}^e	−6.391	−4.611		C^3	−1.088	0.370
	H^A	0.485	0.890	*R*-ptn	H_N^a	−3.513	0.148
	H^B	−0.172	1.153		H_N^e	−5.917	−4.130
	H^C	0.485	0.890		$H^{C,D}$	−0.301	1.939
	H^I	−0.821	1.080		$H^{I,J}$	−1.214	1.265
	H^J	−2.054	2.080		H^M	−0.808	0.225
	H^M	−0.812	0.193		C^1	−3.133	2.530
	C^1	−2.560	1.950		C^2	−2.367	2.367
	$C^{1'}$	−2.560	1.950		C^3	−1.117	0.456
	C^2	−2.267	2.532				
	C^3	−1.088	0.370				

and H_N^e of the 1,2-diamine chelates are 127 (300) and 164 ppm (310 Hz) at 300 K.[10] Almost the same values were observed for H_N^a's of the 1,3-diamine chelates, but H_N^e of the *meso*-ptn chelate exhibited a wide line-width of 840 Hz and resonated at a lower magnetic field by ca. 100 ppm than H_N^e's of the 1,2-diamine chelates.

Geometric Factor. The coordinate system for the analysis of nuclear magnetic resonance is illustrated in Fig. 3, where the z-axis goes through the bonds NC–Fe–CN, and the x-axis bisects the angle N–Fe–N of the six-membered chelate ring. The location of a nucleus relative to the Fe^{III} ion can be represented by the geometric factors (G_A and G_B) defined by the equations $G_A=(3\cos^2\theta-1)/r^3$ and $G_B=\sin\theta\cos 2\phi/r^3$, where the distance r and angles θ and ϕ are defined as shown in Fig. 3.

The geometric factors for the Fe^{III} tn, *meso*-ptn, and *R*-ptn chelates were calculated by assuming that (1) these chelates have the chair, chair, and λ-skew-boat conformations shown in Fig. 1, respectively, and (2) that these conformers have the same geometries as do the complexes, $(-)_{589}$-$[Co(tn)_3Cl_3\cdot H_2O$,[12] $(+)_{510}$-$[Co(meso\text{-}ptn)_2(ox)]ClO_4\cdot H_2O$,[13] $(-)_{546}$-$[Co(R\text{-}ptn)_3]Cl_3\cdot 2H_2O$.[14]

The geometric factors for the 1,3-bn chelate were assumed to be equal to those for the *meso*-ptn chelate. The coordinates of the hydrogen atoms were calculated by assuming that these nuclei locate at the vertices of tetrahedrons with bond lengths of C–H=1.09 and N–H =1.02 Å. These bond lengths were obtained from the neutron diffraction of *trans*-$[CoCl_2(en)_2]Cl\cdot(H_5O_2)^+Cl^-$.[15]

The calculated values of G_A and G_B are listed in Table 2. The values for $H^{A,C}$ and $H^{I,J}$ of the tn chelate were taken to be equal to the mean values for the axial and equatorial protons because the alteration of the tn chelate between two chair conformations rapidly exchanges magnetic atmospheres of these protons. The values for the methyl protons of the *meso*- and *R*-ptn chelates were estimated by assuming a free rotation of the methyl groups.

Analysis of Chemical Shift. The effects of an unpaired electron on the ^1H and ^{13}C NMR shifts can be represented by an isotropic shift (δ^{iso}) defined by the difference in chemical shift between the paramagnetic Fe^{III} complex ($\delta_{Fe^{III}}$) and the diamagnetic Fe^{II} complex ($\delta_{Fe^{II}}$) with the same ligands as the Fe^{III} complex:[8–10]

$$\delta^{iso}=\delta_{Fe^{III}}-\delta_{Fe^{II}} \quad (1)$$

The δ^{iso} values for the *meso*-ptn, tn, *R*-ptn, and 1,3-bn complexes, listed in the sixth column of Table 1, were calculated by assuming that the $\delta_{Fe^{II}}$ values[11] are independent of the temperature.

The N<u>H</u> peak of $[Fe^{II}(CN)_4$ (*meso*-ptn)$]^{2-}$ appeared at 2.16 ppm in pD 2.0 DCl–D_2O.[11] This $\delta_{Fe^{II}}$ value is, however, negligibly small compared to the corresponding $\delta_{Fe^{III}}$ values, and the $\delta_{Fe^{III}}$ values were regarded as the δ^{iso} values for the N<u>H</u>'s.

The δ^{iso} values can be separated into a dipolar shift (δ^{dip}) and a Fermi contact shift (δ^{con}) by using Eqs. 2 and 3:[9,20]

$$\delta^{dip}=(10^6/24\pi)[(2\chi_{zz}-\chi_{yy}-\chi_{xx})\cdot G_A+3(\chi_{xx}-\chi_{yy})\cdot G_B], \quad (2)$$

$$\delta^{con}=10^6 a_N\beta[6k_BT\gamma\hbar\sum_{i=1}^{3}\exp(-E_i/k_BT)]^{-1}\cdot\sum_{q=x,y,z}[\sum_{i=1}^{3}\exp(-E_i/k_BT)\cdot\langle\mu_q\rangle_{ii}-2k_BT\sum_{i=1}^{2}\sum_{j=i+1}^{3}Q_{ij}\ \langle\mu_q\rangle_{ij}\langle s_q\rangle_{ij}]. \quad (3)$$

Here, δ^{dip} and δ^{con} are in units of ppm, and their positive values indicate downfield shifts. The other symbols are defined as reported in a previous paper.[9]

The δ^{dip} values in the seventh column of Table 1 were estimated from Eq. 2. Here, we used the eigenvalues and eigenfunctions of the Kramers doublets obtained for $[Fe^{III}(CN)_4(en)]^-$ because the electronic and CD spectra of the 1,3-diamine complexes resemble those of the 1,2-diamine complex.[11] The δ^{con} values in Table 1 were

Table 3. Fermi Contact Coupling Constants a_N and Spin Population

Diamine	Nucleus	a_N[a] / MHz	$10^4\times$Spin population
tn	H_N	+6.20	+44
	$H^{A,C}$	−0.60±0.03	−4.2±0.2
	$H^{I,J}$	+0.19±0.03	+1.3±0.2
	C^1	+1.32	+4.3
	C^2	−0.19	−0.6
meso-ptn	H_N^a	+2.96	+21
	H_N^e	+9.36	+66
	H^A	+0.11±0.04	+0.8±0.3
	H^I	+0.12±0.04	+0.8±0.3
	H^J	+0.20±0.03	+1.4±0.2
	H^M	−0.07±0.01	−0.5±0.1
	C^1	+1.22	+3.9
	C^2	−0.13	−0.4
	C^3	−0.58	−1.9
1,3-bn	H_{NA}^a	+2.85	+22
	H_{NB}^a	+3.25	+23
	H_{NA}^e	+9.23	+65
	H_{NB}^e	+9.03	+64
	H^A	+0.01	+0.1
	H^B	−0.72	−5.0
	H^C	+0.00	+0.0
	H^I	+0.15	+1.0
	H^J	+0.38	+2.7
	H^M	−0.05	−0.4
	C^1	+1.18	+3.8
	$C^{1'}$	+1.43	+4.6
	C^2	−0.16	−0.5
	C^3	−0.61	−2.0
R-ptn	H_N^a	+4.00	+28
	H_N^e	+7.74	+54
	$H^{C,D}$	−0.50±0.01	−3.5±0.1
	$H^{I,J}$	+0.11±0.03	+0.8±0.2
	H^M	−0.14±0.02	−1.0±0.1
	C^1	+1.22	+3.9
	C^2	−0.13	−0.4
	C^3	−0.45	−1.4

a) Positive a_N indicates that δ^{con} is downfield shift. The a_N values were obtained for CD_3OD solutions containing 0.25% DCl.

obtained by substracting each δ^{dip} value from the corresponding experimental value of δ^{iso}. The Fermi constants in MHz (a_N) calculated from the δ^{con} values by Eq. 3 are summarized in Table 3.

The $\delta_{Fe^{III}}$ values were also estimated from Eqs. 1—3 by employing a_N as a variable so as to obtain the best agreement with the ^1H shifts observed at 323—183 K, and are indicated by the solid lines in Fig. 2. The insufficient agreement for H^A and H^I of the *meso*-ptn chelate is attributable to the use of a single a_N for each nucleus in order to simplify the calculation, although the a_N values vary with the individual terms in Eq. 3.[1,21]

Fermi Contact Shift and Dipolar Shift. The symbols C_α and C_β are used, for convenience, to refer to the carbon atoms in the sequence Fe–N–C_α–C_β. The axial and equatorial protons bonded to the nitrogen and carbon atoms are designated by the symbols H^a_N, H^e_N, H^a_α, H^e_β etc.

(a) Carbon Atoms. The C_α δ^{iso} values for the 1,3-diamine chelates are in the range 165—180 ppm. These δ^{iso}'s are all positive and are ca. 90% of those for the 1,2-diamine chelates.[8–10] Since the δ^{dip} values for C_α are 21—26 ppm, the δ^{iso} values mostly consist of δ^{con}. The estimated δ^{con} values are in the range 144—157 ppm, which have the same sign and are ca. 5% less than those for the 1,2-diamine chelates.[8–10]

The δ^{iso},δ^{dip}, and δ^{con} values for the methyl carbons ($C_{\beta M}$) are in the ranges −40—−63, 6—7, and −53—−69 ppm, respectively, and are ca. 90% of those for the 1,2-diamine chelates with the same sign.[8–10] The central methylene carbons ($C_{\beta C}$) of the 1,3-diamine chelates have δ^{iso} values of 0.8—8 ppm, which differ in both sign and magnitude from those for $C_{\beta M}$ as well as from those for C_β atoms of the 1,2-diamine chelates. This difference is attributed to the small $C_{\beta C}$ δ^{con} values of −15—−22 ppm, which are ca. one fourth of the δ^{con} values for $C_{\beta M}$ and C_β.

(b) CH. The δ^{iso} value for H^A of the *meso*-ptn chelate is about half those for H^a_α of the 1,2-diamine chelates.[8–10] This decrease in δ^{iso} is due to the small δ^{dip} and δ^{con} values for the former.

The δ^{iso} values for H_β, such as H^I and H^J of the *meso*- and *R*-ptn chelates, are ca. 1—3 times as large as those for H_β of the 1,2-diamine chelates. The δ^{con} values for the former comprise 70—80% of the δ^{iso} values, and are 2—3 times as large as the δ^{con} values for the latter. The equatorial H^J has larger δ^{con} values than does the axial H^I. The H^M protons of the *meso*- and *R*-ptn chelates show δ^{iso} values less than half those for the methyl protons of the 1,2-diamine chelates. This is because the former chelates have more negative δ^{con} values than the latter, whereas both chelates have almost the same δ^{dip} values. The δ^{con} values for H^M are opposite in sign to those for H^I and H^J, although these protons belong to the H_β group. Opposite signs of δ^{con} for H^M and $H^{I,J}$ have been reported for paramagnetic Ni^{II} complexes, $[Ni^{II}(H_2O)_4(1,3\text{-diamine})]^{2+}$, with *meso*-ptn, *rac*-ptn, and 1,3-bn.[4]

The negative δ^{iso} value for $H^{A,C}$ of the tn chelate is less than half those for the en chelate with the same sign. This reduction of δ^{iso} is attributed to the small δ^{dip} values for $H^{A,C}$. The δ^{con} value estimated for H^e_α of the 1,3-bn chelate is −21.36 ppm at 300 K, which is similar to the value, −30.2 ppm, estimated from the δ^{con} values for $H^{A,C}$ of the tn chelate and H^A of the *meso*-ptn chelate. These δ^{con} values are 80—90% of those for H^e_α of the 1,2-diamine chelates.[8–10]

(c) NH. The δ^{iso} for amino protons mostly consist of δ^{con} with large negative values. The differences in δ^{iso} between the 1,3- and 1,2-diamine chelates amount to more than 100 ppm for the lower field H^e_N peaks and ca. 20 ppm for the higher field H^a_N peaks.[10] The replacement of the 1,2-diamine chelates by the 1,3-diamine chelates only slightly affects the distances from H^a_N to the *xy* plane (See Fig. 3), such as 0.89—0.95 Å in the former chelates and 0.94—0.97 Å in the latter, whereas the distances with respect to H^e_N are reduced from 0.62—0.76 Å to 0.19—0.34 Å.[12–15,22,23] This correlation between the δ^{iso} values and distances supports the assignment of the amino protons described above.

Spin Population. The nuclei nearer to the *xy* plane showed larger δ^{con} values, as described above. This tendency is ascribed to the unpaired electron predominantly occupying the $3d_{x^2-y^2}$ orbital of the Fe^{III} ion, as has been reported previously for the 1,2-diamine chelates.[9] Since the 1,3-diamine chelates assume chair and/or skew-boat forms, their C_α and $C_{\beta M}$ nuclei are at a distance 0.5—0.6 Å further apart from the *xy* plane than those for the 1,2-diamine chelates with *gauche* forms. The 1,3-diamine chelates thus have smaller δ^{con} values and, accordingly, smaller spin populations than the latter.

The δ^{con} values for C_α and C_β of the 1,3-diamine chelates are opposite in sign, although these values were estimated by neglecting the contribution of ligand-centered dipolar shift (δ_L^{dip}). This suggests that the unpaired spin propagates through σ bonds by a spin-polarization mechanism,[24–26] just as the 1,2-diamine chelates,[8–10] and that the contribution of δ_L^{dip} is small.

The a_N values are related to the spin population in a 1s orbital of hydrogen (Q_{1s}) and that in a 2s orbital of carbon (Q_{2s}) by the relations $Q_{1s}=a_N/1420$ and $Q_{2s}=a_N/3110$, where 1420 and 3110 MHz are Fermi constants calculated for $^1H\cdot$ and $^{13}C\cdot$ radicals, respectively.[27] The estimated values of Q_{1s} and Q_{2s} are listed in Table 3.

The propagation of the positive spin on the Fe^{III} ion by spin-polarization mechanism is expected to give comparable negative spin-populations to both $C_{\beta C}$ and $C_{\beta M}$. However, the δ^{con} value for the former carbon is ca. one third of that for the latter. Since the $C_{\beta C}$ nucleus locates near the *xy* plane and in the direction of the lobe of the $d_{x^2-y^2}$ orbital,[12–14] $C_{\beta C}$ can directly interact with the positive spin in the d orbital (direct mechanism). This interaction yields a positive spin on $C_{\beta C}$, which compensates the negative spin propagated by spin-polarization mechanism, resulting in a decrease in the

negative spin population on $C_{\beta C}$.

The reversal of the sign of δ^{con} between the carbon atoms and protons at the α and β positions indicates that the spin-polarization mechanism is predominant not only in the C–C bonds but also in the C–H bonds. At both the α and β positions, H^e has larger δ^{con} values than H^a. The spin propagation is, thus, anisotropic and occurs more easily in the equatorial direction. This feature is the same as that observed in the 1,2-diamine chelates.[8–10]

Since H^I and H^J of the 1,3-diamine chelates locate in the direction of the lobe of the Fe $d_{x^2-y^2}$ orbital, a direct mechanism is possible for these protons, in addition to the spin-polarization mechanism. Both mechanisms produce a positive spin on these protons, resulting in an increase in their spin populations. The larger δ^{con} values for the H^I and H^J nuclei relative to the values for H_β of the 1,2-diamine chelates are thus attributable to the direct mechanism. The large δ^{con} values for H_N can also be accounted for by the contribution of the direct mechanism.

References

1) J. P. Jesson, "NMR of Paramagnetic Molecules," ed by G. N. La Mar, W. D. Horrocks, Jr., and R. H. Holm, Academic Press, New York (1973), Chap. 1.

2) D. R. Eaton, "NMR of Paramagnetic Molecules," ed by G. N. La Mar, W. D. Horrocks, Jr., and R. H. Holm, Academic Press, New York (1973), Chap. 5.

3) W. D. Horrocks, Jr.,"NMR of Paramagnetic Molecules," ed by G. N. La Mar, W. D. Horrocks, Jr., and R. H. Holm, Academic Press, New York (1973), Chap. 4.

4) J. E. Sarneski and C. N. Reilley, *Inorg. Chem.*, **13**, 977 (1974).

5) C. J. Hawkins and R. M. Peachey, *Acta Chem. Scand., Ser. A*, **32**, 815 (1978).

6) C. E. Strouse and N. A. Matwiyoff, *J. Chem. Soc., Chem. Commun.*, **1970**, 439.

7) I. Morishima, K. Yoshikawa, and K. Okada, *J. Am. Chem. Soc.*, **98**, 3787 (1976).

8) Y. Kuroda, M. Goto, and T. Sakai, *Bull. Chem. Soc. Jpn.*, **60**, 3917 (1987).

9) Y. Kuroda, M. Goto, and T. Sakai, *Bull. Chem. Soc. Jpn.*, **62**, 3614 (1989).

10) Y. Kuroda, M. Goto, and T. Sakai, to be published.

11) M. Goto, H. Nakayabu, H. Ito, H. Tsubamoto, K. Nakabayashi, Y. Kuroda, and T. Sakai, *Inorg. Chem.*, **25**, 1684 (1986).

12) R. Nagao, F. Marumo, and Y. Saito, *Acta Crystallogr., Sect. B*, **29**, 2438 (1973).

13) I. Oonishi, S. Sato, and Y. Saito, *Acta Crystallogr., Sect. B*, **30**, 2256 (1974).

14) A. Kobayashi, F. Marumo, and Y. Saito, *Acta Crystallogr., Sect. B*, **29**, 2443 (1973).

15) J. Rozire and J. M. Williams, *Inorg. Chem.*, **15**, 1174 (1976).

16) Y. Kuroda, M. Goto, and T. Sakai, *Bull. Chem. Soc. Jpn.*, **62**, 3437 (1989).

17) M. Goto, M. Takeshita, N. Kanda, T. Sakai, and V. L. Goedken, *Inorg. Chem.*, **24**, 582 (1985).

18) Y. Kuroda, N. Tanaka, M. Goto, and T. Sakai, *Inorg. Chem.*, **28**, 2163 (1989).

19) The probe temperature was calibrated by the use of the calibration chart supplied by JEOL.

20) Y. Kuroda, N. Tanaka, M. Goto, and T. Sakai, *Inorg. Chem.*, **28**, 997 (1989).

21) R. J. Kurland and B. R. McGarvey, *J. Magn. Reson.*, **2**, 286 (1970).

22) R. Kuroda and Y. Saito, *Acta Crystallogr., Sect. B*, **30**, 2126 (1974).

23) A. Kobayashi, F. Marumo, and Y. Saito, *Acta Crystallogr., Sect. C*, **39**, 807 (1983).

24) Z. Luz, *J. Chem. Phys.*, **48**, 4186 (1968).

25) W. D. Horrocks, Jr. and D. L. Johnston, *Inorg. Chem.*, **10**, 1835 (1971).

26) M. J. Scarlett, A. T. Casey, and R. A. Craig, *Aust. J. Chem.*, **23**, 1333 (1970); **24**, 31 (1971).

27) J. R. Morton, J. R. Rowlands, and D. H. Whiffen, *Natl. Phys. Lab. (U. K.), Rep. BPR*, **1962**, 13.